

A late Holocene paleoclimate reconstruction from Boqueirão Lake sediments, northeastern Brazil



João Cláudio Cerqueira Viana^{a,b,*}, Abdelfettah Sifeddine^{a,b,c}, Bruno Turcq^{b,c},
Ana Luiza Spadano Albuquerque^{a,b}, Luciane Silva Moreira^a,
Doriedson Ferreira Gomes^d, Renato Campello Cordeiro^{a,b}

^a Departamento de Geoquímica, Universidade Federal Fluminense (UFF), Niterói RJ, Brazil

^b Laboratoire Mixte Internationale (LMI), Paleotracés (IRD, Uantof, UFF, UPMC, UPCH), Departamento de Geoquímica, Niterói, Brazil

^c (LOCEAN) – IRD, UPMC, CNRS, MNHN, Centre IRD France Nord, Bondy, France

^d Departamento de Botânica, Universidade Federal da Bahia (UFBA), Salvador, BA, Brazil

ARTICLE INFO

Article history:

Received 21 September 2013

Received in revised form 9 July 2014

Accepted 10 July 2014

Available online 17 July 2014

Keywords:

Diatom-based transfer function

Lake level

ITCZ

MCA

LIA

ABSTRACT

Lake level fluctuations and environmental changes during the late Holocene were inferred from changes in sedimentology, bulk and isotope organic geochemistry, and a diatom based transfer function in a sediment core from Boqueirão Lake, northeast Brazil. The age-depth model was established using fifteen AMS ¹⁴C dates. Lake water level began increasing about AD 400, and reached its maximum during the Medieval Climate Anomaly (MCA), AD ~900–1100. Low lake water level was recorded during the Little Ice Age (LIA), AD ~1400–1820, which allowed macrophyte development in the littoral zone that was recorded by high C_{org}/N_{total} ratios. Considerable lake level variability was evident during the Current Warm Period (CWP). Humid/dry conditions in northeast Brazil during MCA/LIA, respectively, are related to the southward shift of Inter-Tropical Convergence Zone (ITCZ) during austral summer and fall. Those conditions contrast with records of a decrease/increase in the South American Summer Monsoon (SASM) during these periods. This observation also contrasts with paleoclimate inferences from the circum-Caribbean region indicating a northward shift of the ITCZ northern hemisphere summer position during the MCA and a southward shift during the LIA. We suggest that these shifts in ITCZ seasonality were higher during the MCA and smaller during the LIA. Our aim was to answer whether the zonal atmospheric circulation cell between the Amazon and northeast Brazil was responsible for antiphasing with the SASM. A strong monsoon over South America during the LIA reinforced convection upon Amazon, increasing the northeast low in the upper troposphere and large-scale subsidence over northeast Brazil and the Atlantic Ocean leading to a northward repositioning of the South Atlantic Subtropical Anticyclone. These factors in combination may have limited the southward seasonal shift of ITCZ, and they must have been responsible for drier conditions in northeast Brazil during the LIA.

© 2014 Elsevier B.V. All rights reserved.

1. Introduction

The northeast region of Brazil has a dry climate because of the presence of the South Atlantic tropical anticyclone. High interannual climate variability, related to the seasonal shift of the Inter-Tropical Convergence Zone (ITCZ), is responsible for major social and economic consequences in this region. Climate studies (Hastenrath, 1990; Nobre and Shulka, 1996) indicate that this climate variability results in ocean–atmosphere interactions related to tropical Atlantic Dipole.

The dryness in the Brazilian northeast region is influenced by coupling in the upper troposphere between the Bolivian high and the northeast low (Lenters and Cook, 1997; Chen et al., 1999). The Bolivian

high is generated in response to South American monsoon convective precipitation over the Amazon basin, central Andes, and South Atlantic convergence zone (Lenters and Cook, 1997) that creates a circulation cell with an upward branch in Amazonia and southeast Brazil and a large-scale subsidence over the northeast due to the northeast low. The Northeast Low is also influenced by precipitation over Africa (Cook et al., 2004).

The ITCZ is a band of low-level convergence of tradewinds over equatorial oceans that promote a minimum in atmospheric pressure, a low mixed-layer depth, a maximum of Sea Surface Temperature (SST), and deep convective rainfall (Garreaud et al., 2008). A seasonal cycle of rainfall is the main signal of ITCZ influence over northeast Brazil. The ITCZ position depends on tropical Atlantic SSTs (Hastenrath, 1990; Wainer and Venegas, 2002). Anomalous meridional SST gradients and wind stress, relative to the equator, have the dominant control on inter-annual and longer variability over the tropical Atlantic (Nobre

* Corresponding author at: Departamento de Geoquímica, Universidade Federal Fluminense (UFF), Niterói, RJ, Brazil.

E-mail address: jccviana@gmail.com (J.C.C. Viana).

and Shulka, 1996; Melice and Servain, 2003). This variability has a profound impact on total rainfall over northeast Brazil through modulation of the ITCZ latitudinal position (Nobre and Shulka, 1996). For all these reasons, northeast Brazil is sensitive to changes in equatorial wind fields (Hastenrath, 1990).

Tropical Atlantic SSTs and northeast precipitations can be influenced by the El Niño Southern Oscillation (Rodríguez et al., 2011), and at multidecadal time scale the north–south SST gradient is related to the Atlantic Multidecadal Oscillation (AMO) (Knight et al., 2006). The AMO is in turn related to Atlantic Meridional Overturning Circulation (AMOC) (Sutton and Hodson, 2005; Wang and Zhang, 2012). Accordingly, this connection suggests that the ITCZ position may be related to Atlantic thermohaline circulation on longer time scales.

Peterson and Haug (2006) documented the timing and geographic pattern of the ITCZ shift and its impact on late Holocene sub-centennial-scale hydroclimate variability in the Northern Hemisphere. Vuille et al. (2012) suggested that ITCZ shifts controlled the South American Summer Monsoon (SASM) during the last 2000 years. However, reconstructions of ITCZ displacement in northeast Brazil at that time are limited. Zocattelli et al. (2012) identified a wet period between AD 480 and 1380 at Boqueirão Lake, and this phase was followed by a hiatus in sedimentation that lasted almost 500 years. This gap in sediment accumulation may have been a consequence of drier climate. Documenting the time, direction, and magnitude of decadal to centennial changes in ITCZ displacement in the past will help to identify the causes and relative importance of factors that influence ITCZ shifts and improve our knowledge of the climate system in northeast Brazil.

New high-resolution paleoclimate records from tropical South America show that over millennial timescales, orbitally driven factors played a role in ITCZ displacement (Sifeddine et al., 2003; Jacob et al., 2007; Dias et al., 2009). The paucity of high-resolution Holocene paleoclimate records from tropical northeast Brazil, however, has hindered evaluation of ITCZ variability at decadal to centennial timescales. We developed a high-resolution reconstruction of water-level changes

in Boqueirão Lake, northeast Brazil, inferred from a diatom-based transfer function and multiple sediment variables. This paleolimnological record documents sub-decadal to centennial-scale variations in lake level changes over the last 2000 years and provides insights into how the ITCZ South Hemisphere summer position was modulated by North Hemisphere climate conditions during this period.

2. Study area

The Boqueirão Lake is located in Rio Grande do Norte State, Brazil (5°14'42.51"S; 35°32'40.80"W) (Fig. 1). It is an open lake about 6 km long in a NE–SW oriented valley, and its inflow and outflow are by the Boqueirão River, which has a 250 km² basin. The lake has a 350 m average width and a maximum water depth of 10 m. It was formed by damming of the valley of beach ridges, probably during the late Pleistocene (Zocattelli et al., 2012). The lake is polymictic and oligotrophic. Regional climate is tropical sub-humid with 800 to 1200 mm yr⁻¹ annual precipitation that is characterized by a 4-month rainy season from March to June, which is largely influenced by seasonal position of the ITCZ. Modern vegetation ranges from littoral steppe vegetation (*restinga*) to sandy savanna (*cerrado* with *restinga/caatinga* species admixed).

3. Materials and methods

3.1. Coring and sediment sampling

Seismic profiles were obtained in Boqueirão Lake in November 2006 using an ODEC StrataBox™ sediment profiler (Zocattelli et al., 2012). Interpretations of these profiles and information from other sediment cores collected in Boqueirão Lake (Gomes, 2007; Zocattelli et al., 2012) were used to select a new coring site. Boqc0901, a 90-cm-long core, was collected in a water depth of 8.2 m near the center of lake. The Boqc0901 site is 0.7 m deeper than the Boqc0701 site sampled by Zocattelli et al. (2012). The Boqc0901 core was retrieved by divers who

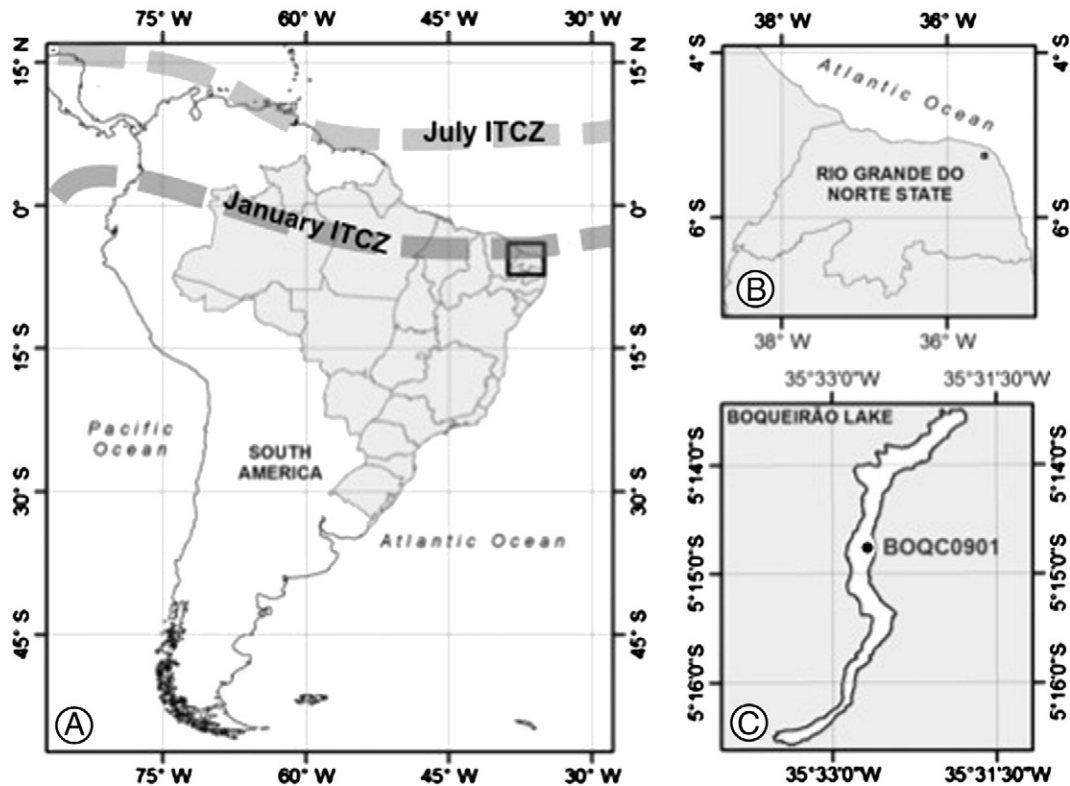


Fig. 1. (A) Location of Boqueirão Lake; (B) State of Rio Grande do Norte, Northeast Brazil; (C) Boqc0901 core site.

used a transparent acrylic core barrel. This core was sampled in the field by slicing into 0.5-cm sections that were stored in plastic bags.

3.2. Radiocarbon chronology and sedimentation rates

The age–depth model is based on fifteen calibrated ^{14}C AMS dates on bulk organic matter, made after carbonate removal (Table 1). Measurements of ^{14}C activity were made by Acceleratory Mass Spectrometry (AMS) at the Laboratoire de Mesure du Carbone 14 (Saclay-France) and NSF AMS Laboratory in Arizona. AMS ^{14}C ages were calibrated using Calib 6.0 software (Stuiver and Reimer, 1993). The calibration curve used was SHcal04 (McCormac et al., 2004). We considered the probability peak of the calibration curve in each 2-sigma (2σ) interval to calculate the age model based on linear regression interpolation.

3.3. Grain-size distributions

The grain-size distribution of the mineral fraction was made after organic matter oxidation with H_2O_2 and dispersion using sodium hexametaphosphate. The grain size of the mineral fraction was measured using a CILAS Particle Analyzer® 1064. The particle size of each sample was rated using the GRADISTAT VERSION 4.0, a grain-size distribution and statistical package for analysis of unconsolidated sediments by laser granulometry (Blott, 2000).

3.4. Bulk and isotopic organic geochemistry

The organic geochemical measurements that were made included total organic carbon (TOC), total nitrogen (TN), $\delta^{13}\text{C}$ (‰) and $\delta^{15}\text{N}$ (‰). We performed analysis of the bulk sediment samples of the Boqc0901 core without acid treatment. The TOC and TN are expressed as percent of total dry sediment weight. The $\text{C}_{\text{org}}/\text{N}_{\text{total}}$ mass ratios were multiplied by the ratio of atomic weights (1.167) of nitrogen and carbon for converting to $\text{C}_{\text{org}}/\text{N}_{\text{total}}$ atomic ratios. The $\delta^{13}\text{C}$ of organic matter is expressed in standard delta notation related to Vienna Pee Dee Belemnite (VPDB). The $\delta^{15}\text{N}$ (‰) of organic matter is expressed related to air standard. TOC and TN analyses on 0.5-cm-thick sediment sections were performed using a CHN auto-analyzer (Perkin Elmer) at the University of California, Davis. Stable isotope measures ($\delta^{13}\text{C}$ and $\delta^{15}\text{N}$) were made by mass spectrometry (Micromass Optima) connected to CHN analyzer.

3.5. Diatom assemblages

Diatoms were analyzed in each 0.5-cm section at 1.0-cm depth intervals in the Boqc0901 core, except between 45 and 40 cm and 25 and 5 cm, where analyses were carried out in every 0.5-cm section to achieve higher temporal resolution for paleoclimate inferences. Diatom extractions from wet sediment were performed using 25% H_2O_2 with $\text{K}_2\text{Cr}_2\text{O}_7$. To dilute the remaining H_2O_2 , samples were then washed with distilled water. The diatom-containing residue was permanently mounted on glass slides with Naphrax® (refraction index = 1.73).

Approximately 400 valves were counted per sample. In a few cases, diatom valves were less abundant and poorly preserved (samples 0–0.5 cm and 1.0–1.5 cm). At least 200 valves were counted in these samples for inclusion in the analysis. Diatoms at each sample were identified to the lowest taxonomic level along random transects, using an Olympus CX31 light microscope. Identification and taxonomy of diatoms were based principally on a database from Boqueirão Lake (Gomes, 2007).

3.6. Diatom-based transfer function

Analysis of the relation between the diatom assemblages in Boqueirão Lake surface-sediment samples and the environmental variables evaluated through a Canonical Correspondence Analysis (CCA) suggests that lake depth is one of the determinants of the structure for the assemblage recorded in modern sediment samples (Gomes et al., 2014). Despite this conclusion, the ratio of λ_1/λ_2 was 0.47, which would indicate an inadequacy in the performance of the transfer function (Gomes et al., 2014). However, according to Velle et al. (2012), the λ_1/λ_2 ratio only indicates the importance of the environmental variable of interest in the calibration-set and a high ratio does not imply that the paleoenvironmental reconstruction is correct.

From the nine explanatory variables used in CCAs, silt, clay, pH, dissolved oxygen and depth were selected as they significantly explained the variability in diatom species data (Gomes et al., 2014). Depth was chosen as one of the variables that explain the distribution of the Boqueirão Lake diatoms. Based on this result, the transfer function was applied to diatom assemblages in the Boqc0901 core to infer past lake water level fluctuations.

The program C2 v1.6.0 (Juggins, 2009) was used to quantitatively reconstruct the changes in water depth (m). A calibration dataset relating thirteen diatom species (relative abundance > 1% in at least one sample) to lake level was constructed using a training set of 66

Table 1

Description of radiocarbon ages obtained on organic matter from bulk sediment of Boqc0901 core (Boqueirão Lake) by AMS Method.

Datation code	Depth interval (cm)	Conventional ^{14}C age (years BP)	Age range (AD/BC)	2-sigma intercept age (cal years AD/BC)
SacA 19130 ^a	10.0–10.5	^b	^b	^b
AA90193 ^c	14.0–14.5	301 ± 40	AD 1611–1674	AD 1640
AA93412 ^c	15.0–15.5	397 ± 37	AD 1456–1626	AD 1500
SacA 19131 ^a	20.0–20.5	530 ± 30	AD 1418–1443	AD 1430
SacA 19132 ^a	30.0–30.5	760 ± 30	AD 1269–1301	AD 1285
SacA 19133 ^a	40.0–40.5	880 ± 30	AD 1157–1267	AD 1215
AA93411 ^c	42.0–42.5	930 ± 37	AD 1148–1210	AD 1175
AA90194 ^c	43.5–44.0	1098 ± 38	AD 894–1042	AD 990
AA93410 ^c	45.0–45.5	1298 ± 38	AD 680–881	AD 775
AA93409 ^c	47.0–47.5	1440 ± 38	AD 620–669	AD 650
acA 19134 ^a	50.0–50.5	1540 ± 30	AD 550–612	AD 590
SacA 19135 ^a	60.0–60.5	1715 ± 30	AD 344–425	AD 405
SacA 19136 ^a	70.0–70.5	1870 ± 30	AD 123–260	AD 230
SacA 19137 ^a	80.0–80.5	2110 ± 30	172 BC–AD 23	50 BC
SacA 19138 ^a	89.5–90.0	2425 ± 30	542 BC–384 BC	400 BC

^a Laboratoire de Mesure du Carbone 14.

^b Activity superior than AD 1950.

^c NSF-Arizona AMS Laboratory.

surface-sediment samples collected along water depth transects on Boqueirão Lake (Gomes, 2007). Six training set samples (e.g. outliers) were excluded from the model before calibration.

Different numerical reconstruction methods were tested for the modern dataset, of which the Weighted Averaging with inverse deshrinking (WA_{inv}) proved to be most appropriate and convincing in the present dataset. The WA_{inv} model had a moderate (1.68 m) root mean squared error of prediction (RMSEP) and predictive power (apparent $r^2 = 0.59$, bootstrapped $r^2 = 0.55$).

4. Results and discussion

4.1. Lithology

The core description (Fig. 2) is derived from grain size distribution and from sediment color based on the Munsell Soil Color Chart. The transparency of the acrylic core barrel allowed color description before the extrusion and sediment slicing. The upper Unit I (0–10 cm) is a fine-sand layer with an increase in clay at the top. Unit II (10–15 cm) is a dark, clayey, fine-sand unit with high clay content (15%). Unit III (15–30 cm) is composed of fine sands with more clay at the base (22–30 cm). Unit IV (30–42 cm) is grayish, silty sand, with more clay at the base. Unit V (42–60 cm) is a fine-sand unit with more clay at the base from 55 to 60 cm. The basal Unit VI (60–90 cm) is a sandy layer that is siltier at the top.

4.2. Chronology

Fifteen AMS radiocarbon dates were obtained on total organic matter in the Boqc0901 core. The radiocarbon ages from Boqc0901 core indicate continuous sedimentation at least for the last 2000 years (Table 1; Fig. 2). Core chronology shows two intervals with low sedimentation rates, one between AD 700 and 1200, which includes the Dark Ages Cold Period (DACP) and MCA event, and another between AD 1550 and 1950, corresponding to the LIA. Three periods of relatively higher sedimentation rate were recorded from 400 BC to AD 500, from AD 1100 to 1500, and during the CWP.

4.3. Grain-size distribution

Unit VI (400 BC–AD 405) is composed of sands (Fig. 3). It contains maximum values of sand-size particles (mean = 63.7%). Sand values decreased at the end of Unit VI (AD 250–405) from a high value of

71.7% to a minimum of 32.8%, as clay and silt content increased (Fig. 3). It may represent a transition between a predominantly erosive environment, suggesting low water-level conditions, to more depositional lake with a high water level.

Higher silt and clay, since the beginning of Unit V (AD 405) until present (Fig. 3) may indicate less-hydrodynamic phases, favoring deposition under deeper-water conditions in Boqueirão Lake. There is a general trend of clay increase that may correspond to a trend toward higher lake levels from AD 405 to present. However, the sandy fraction remains high, around 40% in this phase. The sediment, particularly the sandy fraction, could have been supplied by erosion along the lake margin.

The shoreline near the core site is steep and cuts into Barreiras Formation sediments, which could have supplied the sandy and silty fractions of sediment at the sampling site. In this context, the two phases of slow sedimentation rate between AD 500 and 1100 and between AD 1500 and 1950 could correspond to a more stable lake level whereas the phases of high sedimentation rates would correspond to a more variable lake level that might have been responsible for the erosion of lake margins. The variability of grain size distribution in Unit V to Unit I may indicate occurrences of high runoff and/or strong storm events in the lake.

4.4. Bulk organic matter and its stable isotope characterization

Combined analysis of C_{org}/N_{total} atomic ratio, $\delta^{13}C$ and $\delta^{15}N$ of organic matter can allow distinguishing between phytoplanktonic and vascular plant contributions to sediment organic matter (Meyers and Ishiwatari, 1993; Meyers, 2003; Sifeddine et al., 2004). These variables show abrupt variations that can be used to infer organic matter source and water level. Values of $C_{org}/N_{total} \sim 8$ commonly suggest a phytoplankton source for organic matter, whereas C_{org}/N_{total} ratios ≥ 20 are attributed to the input of macrophytic margin vegetation or terrestrial plant material. The C_{org}/N_{total} ratios in the Boqc0901 core vary from 12.1 to 22.3 and indicate sediment organic matter from multiple sources, along with varying relative contributions. We can observe upwards in the core a general trend toward lower C_{org}/N_{total} ratio (from 18 to 19 to 12 to 14), lower $\delta^{13}C$ (from -23 to -27%) and higher $\delta^{15}N$ (from 0 to 4) that suggests a general trend of more phytoplanktonic contribution that would correspond to a rising lake level in agreement with the trend in clay fraction increase.

Unit VI (400 BC–AD 405) exhibits TOC varying between 13% and 17% and C_{org}/N_{total} values from 17 to 21. In this Unit, $\delta^{13}C$ and $\delta^{15}N$ values are also quite variable, the former varying between -25% and -21% and the latter between -1% and $+3\%$. These variations of all the bulk geochemical parameters may correspond to changes in vegetation types on the lake marginal environment. Values of $\delta^{13}C$, as high as -21% , imply the presence of grasses or other C4 plants near the sampling site.

Unit V (AD 405–1175) is characterized by increases of TOC concentrations from a mean of 16% to $\sim 18\%$. A peak in C_{org}/N_{total} ratio occurs at the beginning of the unit, followed by a sudden decrease, with subsequent values remaining about 15. In this Unit, there is a fairly consistent decline in $\delta^{13}C$ from about -22% to -23% . Just above the unit base, $\delta^{15}N$ increases abruptly from near 0‰ to 4‰ and shows a second increase to 6‰ at the top of the unit. All these parameters suggest a deeper lake at that time, with higher phytoplanktonic contribution and lower macrophytic organic matter sources as recorded by the lower C_{org}/N_{total} values.

In Unit IV (AD 1175–1285), TOC values remain high, around 18%. The $\delta^{13}C$ continues decreasing, from -23% to -25% . In contrast, the $\delta^{15}N$ (‰) values fluctuate, varying from $+8\%$ to 0‰. The high TOC content probably indicates a lake still high at this time (Turcq et al., 2002).

In Unit III (AD 1285–1500), TOC concentration decreases from about 18% to 12%, while C_{org}/N_{total} shows low values at the base of the unit (~ 14), but increases suddenly in the middle of the unit, reaching values around 19. The $\delta^{13}C$ continues to decrease slightly, declining from about

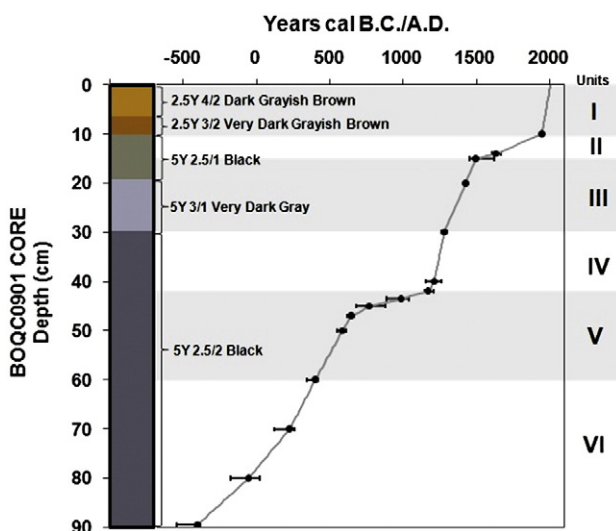


Fig. 2. Plot of measured ages vs. depth for the Boqc0901 core. Units are represented with horizontal white and gray markings.

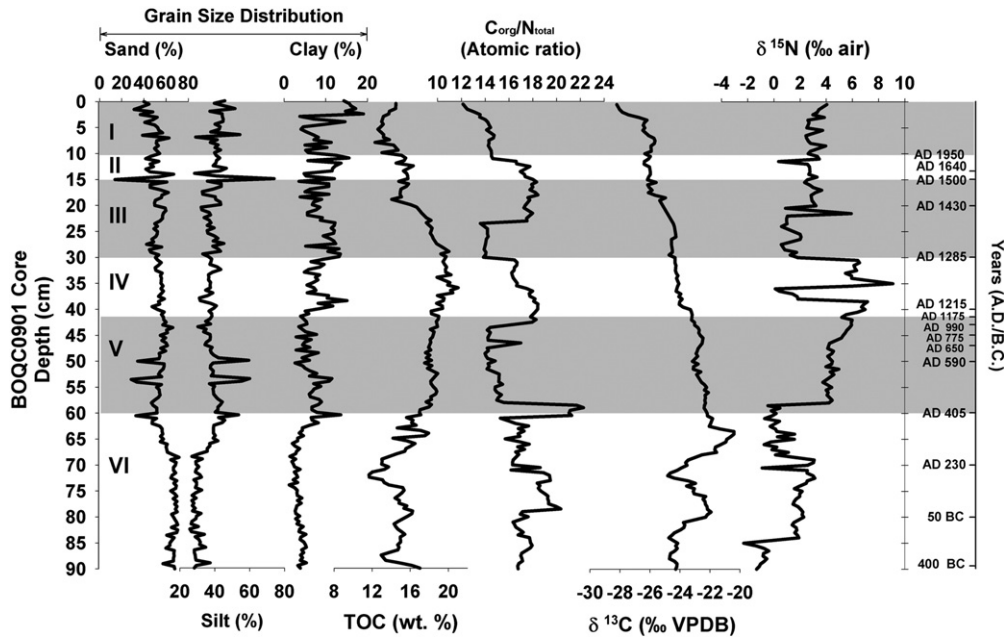


Fig. 3. Description of the Boqc0901 core, grain size distribution, Total Organic Carbon (TOC), C/N, $\delta^{13}\text{C}$ and $\delta^{15}\text{N}$. Units are represented with horizontal white and gray markings.

–24‰ to –26‰ at the top of the unit. The $\delta^{15}\text{N}$ values at the base of this unit display an abrupt decrease from about +6 to +1‰, but rise again to about +3‰ in the upper half of the unit. The lower TOC content and high $C_{\text{org}}/N_{\text{total}}$ could correspond to a lower lake level with more macrophytic contributions.

In Unit II (AD 1500–1950) and Unit I (AD 1950 until recent decades), $\delta^{15}\text{N}$ remains relatively stable, varying about a mean of +3‰, as does TOC content (14%), $\delta^{13}\text{C}$ (–27‰) and the $C_{\text{org}}/N_{\text{total}}$ ratio (18), although the latter parameter decreases somewhat at the top of the unit. The general stability of this unit suggests that the lake level remained low during this period.

In Unit I, $C_{\text{org}}/N_{\text{total}}$ ratio and $\delta^{15}\text{N}$ increase to almost 12 and 4‰ respectively while $\delta^{13}\text{C}$ decreases to –29‰. These changes suggest a new increase in phytoplanktonic productivity that may be due to a higher lake level.

4.5. Diatom assemblages

In Unit VI (400 BC–AD 405), relative abundances of *Mastogloia smithii* var. *lacustris* Lange-Bertalot remained below 50%. Indeed, at the end of Unit VI (AD 220–405) *Nitzschia amphibia* Grunow at some times shows higher values than *M. smithii* var. *lacustris* (Fig. 4). The presence of *Brachysira brebissonii* Ross (acidobiontic: optimal pH < 5.5) in Unit VI may represent a period of more acid waters in Boqueirão Lake. Acid waters may indicate large amounts of organic matter decomposition at the margins of the lake.

The sudden and extreme reduction in relative abundances of *B. brebissonii* (0%) and *N. amphibia* (6.1%) at the end of Unit VI may reflect a shift in water conditions, specifically, an increase in pH. This, in turn, may reflect a reduction in the influence of marginal macrophyte vegetation because of an increase in water level.

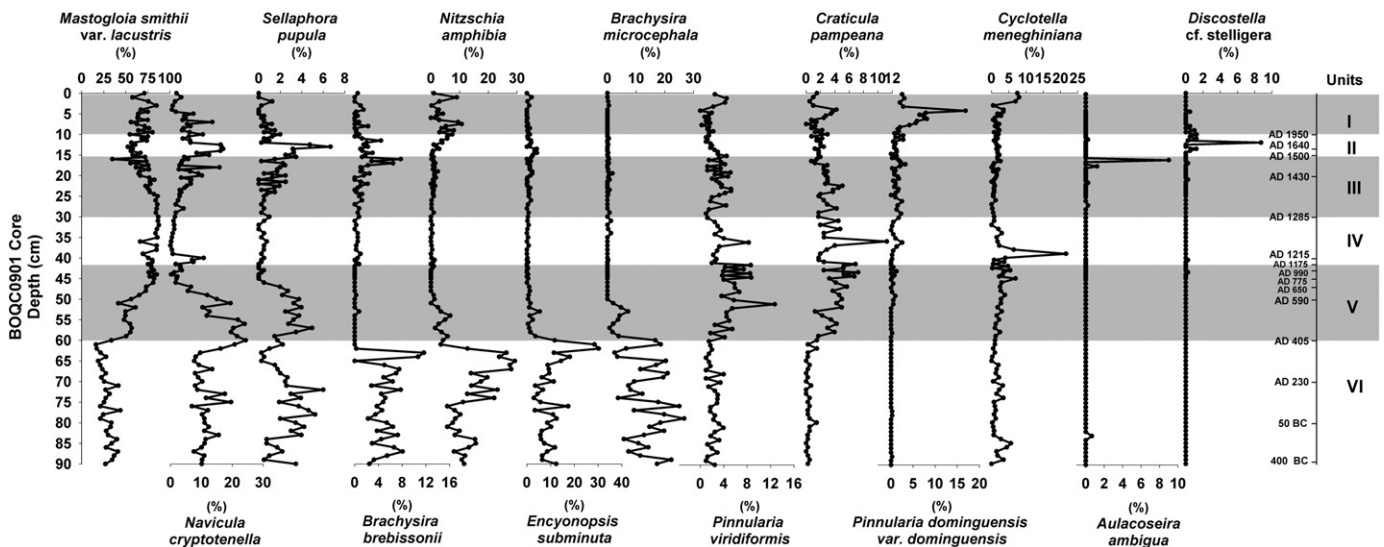


Fig. 4. Relative abundances (%) of main diatom species along the Boqc0901 core. Units are represented with horizontal white and gray markings.

The initial part of Unit V (AD 405–430) highlights the beginning of important paleolimnological changes in Boqueirão Lake from the initial growth in relative abundance and later dominance (50.5%) of *M. smithii* var. *lacustris*. These shifts imply a higher pH and lower nutrients, especially phosphorus. Dominance of *M. smithii* var. *lacustris* suggests more oligotrophic conditions in Boqueirão Lake because this taxon responds negatively to high concentrations of phosphorus and prefers alkaline conditions (Gaiser et al., 2006). If the margin of the lake contributes to organic matter and leads to low pH, indicating shallower water, the shift to higher pH is thought to reflect rising water level.

In the middle of Unit V (AD 430–700) the *N. cryptotenella* values decrease to ~2% and *M. smithii* var. *lacustris* increases its dominance over 80% (the highest value previously recorded). After abrupt reductions at the Unit VI/Unit V boundary, *B. microcephala* (Grunow) Compère is absent after AD 590 and *N. amphibia* disappears from records at AD 630 (Fig. 4). The absence of *N. amphibia* may indicate less eutrophic conditions in Boqueirão Lake, and frequent absences of *B. brebissonii* may correspond to less acidic conditions. The decrease in productivity could lead to a decrease in organic matter degradation in the water column, higher dissolved CO₂ content and higher pH. These proposed conditions are different from those recorded in previous units.

The peak of *Cyclotella meneghiniana* Kützing occurs in Unit IV (AD 1220). The end of Unit V and beginning of Unit IV (AD 1250–1380) display relative abundances of *M. smithii* var. *lacustris* >80%, with the highest value in AD 1270 (87.4%). In AD 1370–1380 relative abundance of this taxon declined, which is interpreted to indicate loss of deeper habitats.

Within Unit III and Unit II (AD 1380–1830), relative abundances of *M. smithii* var. *lacustris* declined (minimum 34.8% around AD 1490), which may indicate a decrease in water level. *B. brebissonii* showed a peak of 7.8%, and *Discostella* cf. *stelligera* (Cleve & Grunow) Houk & Klee displayed a peak of 9%. Favorable conditions for the reappearance of *B. brebissonii*, mainly in reduced water pH, are thought to be a consequence of shallower environments with decomposition of macrophytes in the littoral zone. The presence of *Discostella* cf. *stelligera*, a planktonic diatom that is favored by periods of thermal stratification, suggests a deeper water level even though the water level has decreased in Boqueirão Lake. Deeper water would increase the amount of open-water habitat, favoring planktonic/tychoplanktonic species (Ruhland et al., 2003; Tingstad et al., 2011).

Aulacoseira ambigua (Grunow) Simonsen var. *ambigua* first appeared about AD 990. This taxon was recorded again at AD 1210, 1420 and 1470. The relative abundances were typically only between 1% and 1.3% about AD 1680, 1870, 1950 and 1960. However, there is a peak of 8.8% about AD 1800. *A. ambigua* var. *ambigua* suggests turbulent water conditions induced by wind, and it is often observed in polymictic environments (Reynolds, 1993; Pérez et al., 1999).

4.6. Diatom-based transfer function

The transfer function was based on thirteen taxa: *M. smithii* var. *lacustris* Grunow, *Navicula cryptotenella* Lange-Bertalot, *N. amphibia* Grunow, *C. meneghiniana* Kützing, *B. brebissonii* Ross, *Sellaphora pupula* (Kützing) Mereschkowsky, *Encyonema silesiacum* (Bleisch) Mann, *Pinnularia domingensis* (P.T. Cleve) Husted var. *domingensis*, *Pinnularia viridiformis* Krammer, *Amphora copulata* (Kützing) Schoeman & Archibald, *Staurosirella* cf. *pinnata* (Ehrenberg) Williams & Round, *Ulnaria ulna* (Nitzsch.) Compère and *A. ambigua* (Grunow) Simonsen var. *ambigua*. These taxa represent 87.3% of total species from the Boqc0901 core.

The Boqueirão Lake water level reconstruction (Fig. 5) shows four major phases: (1) Lower water levels were recorded between ca. 400 BC and AD 350, with minimum depth around AD 350 (3.62 ± 1.73 m); (2) lake level increase began at AD 390 (5.13 ± 1.74 m) and another less prominent rise between AD 460 and AD 550, reaching a maximum during the MCA (AD 900 and 1100) at AD 920 (7.65 ± 1.76 m); (3) a slow lake-level decrease started during the transition period between the MCA and the LIA with many fluctuations. The LIA was marked by the lowest lake level recorded during the last 1000 years (AD 1720: 5.42 ± 1.67 m); (4) Lake level increased again beginning at AD 1830 and increased abruptly during the CWP (max: 7.22 ± 1.68 m), when it reached again the level achieved during the MCA.

4.7. Relations between lake level fluctuations and sedimentary characteristics

The general trend of a lake level rise, suggested by the grain size distribution (clay increase) and bulk and isotope organic matter parameters (C_{org}/N_{total} and δ¹³C decrease and δ¹⁵N increases), is confirmed by diatom-based transfer function although the lake level (Fig. 5) exhibits marked fluctuations during this general rising trend.

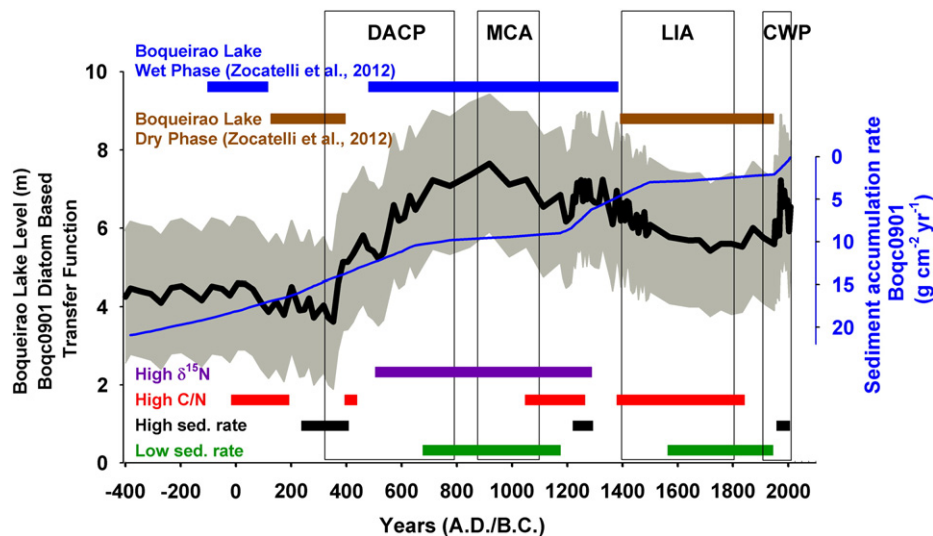


Fig. 5. Changes in water depth (m) inferred from the diatom-based transfer function (Boqc0901) and sediment accumulation rate ($\text{g cm}^{-2} \text{ years}^{-1}$). Relatively errors Root Mean Squared Error of Prediction (RMSEP) are represented by gray scale. Bars show high C/N (red bars), high $\delta^{15}\text{N}$ (purple bar), low sedimentation rate (green bars) and high sedimentation rate (black bars) from core Boqc0901; and wet (blue bars) and dry phases (brown bars) from core Boqc0701 (Zocatelli et al., 2012). DACP: Dark Age Cold Period; MCA: Medieval Climate Anomaly; LIA: Little Ice Age; and CWP: Current Warm Period.

Two phases of low sedimentation rate were observed in the core, from AD 700 to 1200 and from AD 1550 to 1950 (Fig. 2). Zocatelli et al. (2012) observed almost the same phases in the Boqc0701 core, the last one corresponding to a complete interruption of sedimentation (hiatus). The low sedimentation phase began one or two centuries earlier in Boqc0701 than in the Boqc0901 core because Boqc0901 is 70 cm deeper. A comparison between sedimentation rates and lake level variations indicates that high sedimentation rates correspond to lake level variations, whereas the low sedimentation rates are associated with stable levels, being high for the AD 700–1200 phase and low during the AD 1550–1950 phase. This relation is due to location of the core site, which is away from the small river sediment supply. At this point, the sedimentary supply comes mainly from margin erosion. This erosion is higher during episodes of lake level rise than during stable or decreasing level phases.

In Fig. 5, we compare the lake level curve reconstructed from diatom-based transfer function to C_{org}/N_{total} values in the core (Fig. 3). The intervals of high C_{org}/N_{total} values seem not to be related to the delivery of detrital organic matter because they show no relation to quality (e.g. clay content) and quantity of sediment supply (sedimentation rate and accumulated rates). Instead, these higher C_{org}/N_{total} intervals are interpreted as phases of higher contribution of macrophytes to the sediment organic matter. They correspond to phases of lower lake water level that favored macrophyte development. One exception is the short episode of very high C_{org}/N_{total} around AD 400, which corresponds to the beginning of a lake level rise. Comparison from C_{org}/N_{total} ratio with $\delta^{13}C$ and $\delta^{15}N$ values (Fig. 5) indicates changes in the sedimentary organic matter (SOM) characteristics. The high C_{org}/N_{total} phase at the base of the core in unit VI corresponds to the higher values of $\delta^{13}C$ and lower values of $\delta^{15}N$. The less negative $\delta^{13}C$ could correspond to a higher contribution of C4 plants to the macrophytic community or to land plants around the margin of lake. An increase of the algal contribution is another possibility. Although the C_{org}/N_{total} ratio indicates a higher macrophytic contribution, epiphytic and periphytic algae may follow macrophyte development (e.g. Boussafir et al., 2012). After the C_{org}/N_{total} ratio peak at AD 400, there was an abrupt increase in $\delta^{15}N$, indicating that the water level rise provoked a complete change in the biogeochemical processes functioning in the lake, with more nutrient cycling and probably more planktonic production. The TOC concentration (Fig. 3) is higher during the high-level phase (Fig. 5). This phenomenon is frequently observed in Brazilian lakes (Turcq et al., 2002) and could be due to a higher supply of land-derived nutrients and/or less intense organic matter degradation during high-level phases.

If we compare the past lake water level fluctuations with the interpretations of Zocatelli et al. (2012) there is a general agreement related to the periods (Fig. 5), the main difference being the phase between 100 BC and AD 120, which Zocatelli et al. (2012) considered to have been as humid as the phases that followed. In our lake level reconstruction, there is a relatively humid phase before AD 300. The development of macrophytes (high C_{org}/N_{total}) probably occurred at the end of this phase and during the subsequent lake-level lowering, which explains the good SOM preservation observed by Zocatelli et al. (2012). Before AD 300, diatom assemblages were very different from those during the highest water level phases after AD 300. Presences of planktonic/tychoplanktonic species suggest deeper waters in Boqueirão Lake, whereas acidobiontic species suggest phases of shallow lake. Diatom assemblages are probably more sensitive than bulk organic matter variables used by Zocatelli et al. (2012) for inferring past lake water level.

4.8. Paleoclimate evidence

Seasonal climate of northeast Brazil is currently mainly controlled by shifts in the position of the ITCZ. Different interacting drivers influence the amount and distribution of rainfall at decadal, multidecadal and centennial timescales. At the inter-annual timescale, the tropical Atlantic Dipole influences these shifts and the AMO at a multidecadal

timescale. ENSO also has an influence, expressed as prolonged dry and rainy seasons during El Niño and La Niña periods, respectively (Melice and Servain, 2003). However, causes for past climate variability in northeastern Brazil during the last 2000 years are poorly studied. Several reconstructions of SST in the Indo-Pacific region indicate La Niña conditions during the MCA (Mann et al., 2009) and El Niño conditions during the LIA (Cobb et al., 2003), but these are difficult to reconcile with changes influencing northeastern Brazil at the regional scale. Recent studies suggest that prolonged North Atlantic SST anomalies (Bird et al., 2011) influenced changes in South American Summer Monsoon (SASM) activity and consequently the displacement of the ITCZ during the last 1000 years. Vuille et al. (2012) also suggested that the southern position of the ITCZ during the LIA forced a more intense SASM.

Our results show that the DACP (ca. AD 300 to 800) and the LIA were marked by low water levels in Boqueirão Lake. Before the DACP, from ca. 400 BC to AD 350, a period existed when the lake received less rainfall. Thereafter, the limnological characteristics change during a period of rising water level (ca. AD 350–650) that is inferred from the diatom-based transfer function. This period overlaps the DACP cold event in the North Atlantic region. Cold events in the Northern Hemisphere can shift the ITCZ toward a more southern position (Bird et al., 2011; Vuille et al., 2012) but we have evidence for an opposite tendency for dryer climate in northeast Brazil in the Boqueirão record.

4.8.1. Medieval Climate Anomaly – MCA (AD ~900–1100)

The humid conditions in Boqueirão Lake (5°S) for the MCA, inferred mainly from organic parameters and the diatom-based transfer function, might be related to a persistent negative phase of the Atlantic Multidecadal Oscillation (AMO) during the MCA. However, they do not fit with evidence for a warmer climate in the North Atlantic (e.g. Mann et al., 2005).

Below-normal rain in northeast Brazil during the rainy season is usually related to periods of abnormal warming of waters in the tropical North Atlantic sector, which occurs when the position of the ITCZ is shifted to the north and/or when the conditions of El Niño prevail in the tropical Pacific (Hastenrath, 2000). High titanium concentrations in a sediment core from the Cariaco Basin (~10°N) during the MCA support the inference for northward migration of the ITCZ (Haug et al., 2001). Our results suggest, however, that the ITCZ also remained in a southerly position (~5°S) during the MCA. The northward ITCZ position corresponds to northern hemisphere summer (July–September), whereas our data indicate that the ITCZ was in a southerly position during southern hemisphere autumn (March to May). The different records suggest that the seasonal ITCZ latitudinal shift was larger at that time.

Interannual variations in modern SASM are caused by a number of factors such as SST anomalies in the Pacific associated with the ENSO, which modulates the variability in SASM, leading to changes in Walker and Hadley circulation in South America. Changes in SST in the tropical Atlantic have been related to inter-annual variations in the activity of SASM and drought conditions in the Amazon Basin (Bird et al., 2011). Thus, a strong SASM could reinforce the South Atlantic Subtropical Anticyclone, leading to dry conditions in northeast Brazil, with the opposite occurring during a weak monsoon phase (Cruz et al., 2009). Sediment records ($\delta^{18}O$ cal) from Laguna Pumacocha, a high-altitude lake in the eastern Peruvian Andes (~10°S), suggest that the SASM was considerably reduced during the MCA, which may have induced more rainfall in northeast Brazil, supporting our interpretation (Fig. 6).

4.8.2. Little Ice Age – LIA (AD ~1400–1820)

The primary mechanism proposed to explain the decrease in circum-Caribbean precipitation during the LIA, is a decrease in the intensity of the ITCZ annual cycle and a displacement of the ITCZ to the south (Hodell et al., 2005). Moreover, the reduction in Atlantic Meridional Overturning Circulation (AMOC) and expansion of ice in the North Atlantic would force this ITCZ southern shift (Haug et al., 2001). The

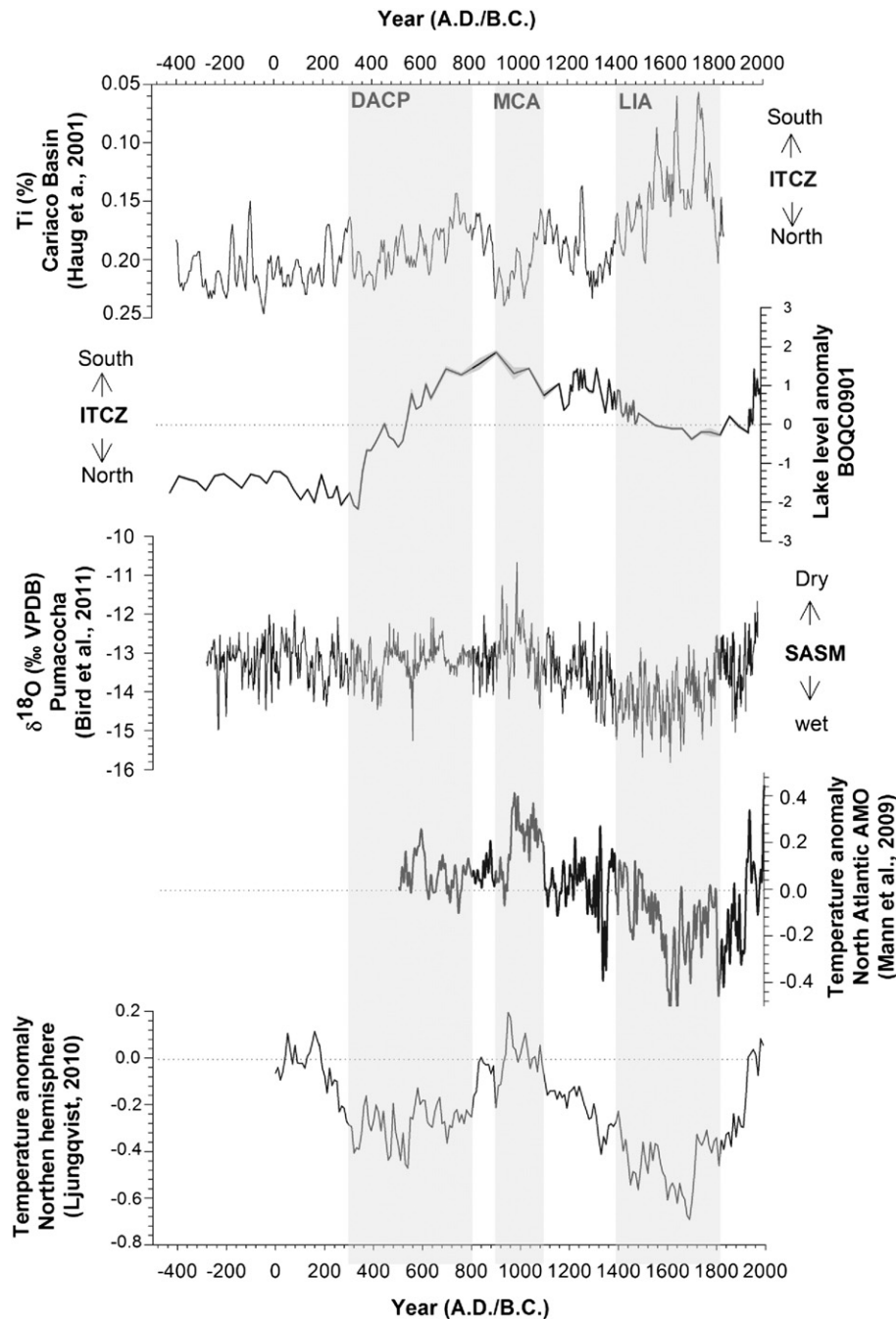


Fig. 6. Comparison among Ti anomaly from Cariaco Basin (Haug et al., 2001), Boqueirão Lake level reconstruction, $\delta^{18}\text{O}$ from Pumacochoa (Bird et al., 2011), Temperature Anomaly (Mann et al., 2009) and temperature reconstruction NH (Ljungqvist, 2010).

LIA cooling, especially during the seventeenth century, appears to be more severe than the cooling during the Dark Ages Cold Period (Ljungqvist, 2010). Cooling in the Northern Hemisphere during the LIA and weakening of the AMOC could have influenced the displacement of the ITCZ to the south, as suggested by paleoclimate studies and climate models (Mann, 2002; Sifeddine et al., 2008; Licciardi et al., 2009; Ran et al., 2011).

In the circum-Caribbean region, a decrease in titanium (Ti) concentration in Cariaco Basin ($\sim 10^\circ\text{N}$) sediment suggests reduced rainfall (increased aridity) in this area during the LIA between AD ~ 1400 and 1750 (Haug et al., 2001). $\delta^{18}\text{O}$ and Mg/Ca from coral records in the Caribbean Sea ($\sim 19^\circ\text{N}$) show a tag in the LIA expressed as a decrease in SST (Watanabe et al., 2001). On the Yucatan Peninsula, an ostracod $\delta^{18}\text{O}$

record from Aguada X'caamal suggests arid conditions during the LIA, especially during the middle of the 15th century (Hodell et al., 2005).

Vuille et al. (2012) suggested that the more southern position of ITCZ was the driver of drier conditions observed in Amazonia during the LIA. Our data, however, show that ITCZ was at a more northern position during Southern Hemisphere summer and fall because Boqueirão Lake displayed very low water level at that time. The same lake condition has also been concluded by Zocatelli et al. (2012), using other proxies. It seems that during the LIA, a strong SASM probably reinforced the South Atlantic Subtropical Anticyclone, limiting the southward shift of the ITCZ and bringing drier conditions to northeast Brazil, a mechanism already suggested for the early and middle Holocene (Cruz et al., 2009) and during the late Holocene (Novello et al.,

2012). These conditions might explain the dry phase we observed in northeast Brazil during the LIA (Fig. 6).

5. Conclusions

The sediment record from Boqueirão Lake provides information on paleoclimate variability in northeast Brazil during the last two millennia, with clear inferences for conditions during the Dark Ages Cold Period, the Medieval Climate Anomaly and the Little Ice Age. Changes in C/N ratios, sediment particle sizes, and relative abundances of diatoms during this period are attributed to shifts in the position of the ITCZ during Southern Hemisphere summer and fall, which are primarily responsible for rainfall at Boqueirão Lake.

Boqueirão Lake water level was low between ca. 400 BC and AD 300, and minimum depth occurred around AD 300. Lake level began to increase starting at AD 335, reaching its maximum at the beginning of the MCA, between AD 900 and 1100. A high lake level is recorded by finer particles in the inorganic fraction (silt and clay), low C_{org}/N_{total} ratios, occurrence of planktonic taxa (e.g. *Discostella cf. stelligera*), oligotrophic diatom taxa (e.g. *M. smithii* var. *lacustris*), and by the application of a diatom-based transfer function for inferring past lake-level. Lake level decreased during the transition period between the MCA and the LIA, and the lowest lake level of the last 1000 years occurred about AD 1700. Lake level began to increase again during the last century and reached a level equivalent to the MCA peak.

Climate in the Boqueirão Lake region is very sensitive to ITCZ position. The lake level changes we inferred contrast with the commonly accepted paradigm that warm conditions in the Northern Hemisphere pushed the ITCZ to the north, whereas cold conditions in the Northern Hemisphere forced a southward shift of the ITCZ. During the MCA (warm conditions in the Northern Hemisphere), the lake (5°S) was at its highest level, whereas during the LIA (cold Northern Hemisphere) the lake record shows its lowest water level of the last 1000 years. In addition to the indications of ITCZ position during northern hemisphere summer (e.g. Haug et al., 2001), we conclude that ITCZ seasonal shifts were larger during the MCA and smaller during the LIA.

Our hypothesis is that the climate in northeast Brazil was influenced by the South American Summer Monsoon during these phases. A weaker monsoon during the MCA led to a weakening of the South Atlantic Subtropical Anticyclone, allowing the ITCZ to reach northeast Brazil during the Southern Hemisphere summer and autumn, whereas during the Northern Hemisphere summer, the ITCZ was shifted northward. During the LIA, the reverse occurred – a high-intensity South American Summer Monsoon amplified the South Atlantic Subtropical Anticyclone, which could have limited the southward shift of the ITCZ, leading to drier conditions in northeast Brazil, whereas during the Northern Hemisphere summer the ITCZ was shifted to the south, probably due to cold conditions in the Northern Hemisphere. The seasonal succession of coupled ocean/atmosphere mechanisms that led to this observed difference between MCA and LIA merit further investigations, employing both more measurements and more model simulations.

Acknowledgments

This work was supported by the Department of Geochemistry of the Universidade Federal Fluminense-UFF (Brazil), Universidade Federal da Bahia-UFBA (Brazil), and LOCEAN (IRD-Sorbonne Université/UPMC/CNRS/MNHN) and LMI Paleotracas (IRD/UPMC/Uantof/UFF/UPCH). We acknowledge financial support from the project PRIMO project (CNPq/IRD: CNPq-590172/2011-5), the ANR ELPASO (2010 blanc 60801) and the “Laboratoire de mesure du Carbone 14” LMC14 (UMS 2572, CEA-CNRS-IRD-IRSN-Ministère de la Culture), Gif-sur Yvette, France, through the IRD financial and technical support to this laboratory. We also thank to Eduardo Mendes da Silva, Marlene Campos Peso de Aguiar, Denise de Campos Bicudo, Francisco Willian da Cruz Junior and Philip Meyers for their assistance at different stages of this

work. We are especially grateful to Mark Brenner and a second reviewer for their constructive and helpful suggestions to improve this contribution.

References

- Bird, B.W., Abbott, M.B., Vuille, M., Rodbell, D.T., Stansel, N.D., Rosenmeier, M.F., 2011. A 2,300-year-long annually resolved record of the South American summer monsoon from the Peruvian Andes. *PNAS*. <http://dx.doi.org/10.1073/pnas.1003719108> (Early edition).
- Blott, S., 2000. GRADISTAT Version 4.0: A Grain Size Distribution and Statistics Package for the Analysis of Unconsolidated Sediments by Sieving or Laser Granulometer. Surface Processes and Modern Environments Research Group, Department of Geology, Royal Holloway University of London (Available at <http://www.kpal.co.uk/gradistat.html>).
- Boussafir, M., Sifeddine, A., Jacob, J., Foudi, M., Cordeiro, R., Albuquerque, A.L.S., Abrão, J., Turcq, B., 2012. Petrographical and geochemical study of modern lacustrine sedimentary organic matter (Lagoa do Caçô), Maranhão, Brazil): Relationship between early diagenesis, organic sedimentation and lacustrine filling. *Org. Geochem.* 47, 88–98.
- Chen, T.C., Weng, S.P., Shubert, S., 1999. Maintenance of Austral Summertime upper-tropospheric circulation over tropical South America: the Bolivian High–Nordeste Low System. *J. Atmos. Sci.* 56, 2081–2100.
- Cobb, K.M., Charles, C.D., Cheng, H., Edwards, R.L., 2003. El Niño/Southern Oscillation and tropical Pacific climate during the last millennium. *Nature* 424, 271–276.
- Cook, K.H., Hsieh, J.S., Hagos, S.M., 2004. The Africa–South America intercontinental teleconnection. *J. Clim.* 17, 2851–2865.
- Cruz, F.W., Vuille, M., Burns, S.J., Wang, X., Cheng, H., Werner, M., Edwards, R.L., Karmann, I., Auler, A.S., Nguyen, H., 2009. Orbitally driven east–west antiphasing of South American precipitation. *Nat. Geosci.* 2, 210–214.
- Dias, P.L.S., Turcq, B., Dias, M.A.F.S., Braconnot, P., Jorgetti, T., 2009. Mid-Holocene climate of tropical South America: a model–data approach. *Past Climate Variability in South America and Surrounding Regions. Developments in paleoenvironmental research*, 14, pp. 259–281.
- Gaiser, E.E., Richards, J.H., Trexler, J.C., Jones, R.D., Childers, D.L., 2006. Periphyton responses to eutrophication in the Florida Everglades: cross-system patterns of structural and compositional change. *Limnol. Oceanogr.* 51, 617–630.
- Garreaud, R.D., Vuille, M., Compagnucci, R., Marengo, J., 2008. Present-day South American climate. *Palaeogeogr. Palaeoclimatol. Palaeoecol.* 281 (3–4), 180–195.
- Gomes, D.F., 2007. Elaboração de funções de transferência para a reconstrução de paleoprofundidade na lagoa do Boqueirão – RN – com base em diatomáceas (Ph.D Thesis) Universidade Federal Fluminense, Brazil.
- Gomes, D.F., Albuquerque, A.L.S., Torgan, L.C., Turcq, B., Sifeddine, A., 2014. Assessment of a diatom-based transfer function for the reconstruction of lake-level changes in Boqueirão Lake, Brazilian Nordeste. *Palaeogeogr. Palaeoclimatol. Palaeoecol.* 415, 105–116.
- Hastenrath, S., 1990. Prediction of Northeast Brazil rainfall anomalies. *J. Clim.* 3, 893–904.
- Hastenrath, S., 2000. Interannual and longer-term variability of upper-air circulation in the Northeast Brazil Tropical Atlantic Sector. *J. Geophys. Res.* 105, 7327–7335.
- Haug, G.H., Hughen, K.A., Sigman, D.M., Peterson, L.C., Röhl, U., 2001. Southward migration of the intertropical convergence zone through the Holocene. *Science* 293, 1304–1308.
- Hodell, D.A., Brenner, M., Curtis, J.H., Medina-Gonzalez, R., Rosenmeier, M.F., Can, E.L.C., Albornaz-Pat, A., Guilderson, T.P., 2005. Climate change on the Yucatan Peninsula during the Little Ice Age. *Quat. Res.* 63, 109–121.
- Jacob, J., Huang, Y., Disnar, J.R., Sifeddine, A., Boussafir, M., Albuquerque, A.L.S., Turcq, B., 2007. Paleohydrological changes during the last deglaciation in Northern Brazil. *Quat. Sci. Rev.* 26, 1004–1015.
- Juggins, S., 2009. C2 User Guide, Version 1.6.0. Software for Ecological and Palaeoecological Data Analysis and Visualization. University of Newcastle. Newcastle upon Tyne, England.
- Knight, J.R., Folland, C.K., Scaife, A.A., 2006. Climate impacts of the Atlantic Multidecadal Oscillation. *Geophys. Res. Lett.* 33, L17706. <http://dx.doi.org/10.1029/2006GL026242>.
- Lenters, J.D., Cook, K.H., 1997. On the origin of the Bolivian high and related circulation features of the South American climate. *J. Atmos. Sci.* 54, 656–677.
- Licciardi, J.M., Schaefer, J.M., Taggart, J.R., Lund, D.C., 2009. Holocene glaciers fluctuations in the Peruvian Andes indicate northern climate linkages. *Science* 325, 1677–1679.
- Ljungqvist, F.C., 2010. A new reconstruction of temperature variability in the extra-tropical Northern Hemisphere during the last two millennia. *Geogr. Ann. Ser. A* 92, 339–351.
- Mann, M.E., 2002. Little Ice Age. In: MacCracken, Michael C., Perry, J.S. (Eds.), *The Earth system: physical and chemical dimensions of global environmental change. Encyclopedia of Global Environmental Change*, pp. 504–509.
- Mann, M.E., Rutherford, S., Wahl, E., Ammann, C., 2005. Testing the fidelity of Methods Used in Proxy-Based Reconstruction of Past Climate. *J. Clim.* 18, 4097–4107.
- Mann, M.E., Zhang, Z., Rutherford, S., Bradley, R., Hughes, M.K., Shindell, D., Ammann, C., Faluvegi, G., Ni, F., 2009. Global signatures and dynamical origins of the Little Ice Age and Medieval Climate Anomaly. *Science* 326, 1256–1260.
- McCormac, F.G., Hogg, A.G., Blackwell, P.G., Buck, C.E., Higham, T.F.G., Reimer, P.J., 2004. SHCal04 Southern Hemisphere Calibration 0–11.0 cal kyr BP. *Radiocarbon* 46, 1087–1092.
- Melice, J.L., Servain, J., 2003. The tropical Atlantic meridional SST gradient index and its relationships with the SOI, NAO and Southern Ocean. *Clim. Dyn.* 20 (5), 447–464.
- Meyers, P., 2003. Applications of organic geochemistry to paleolimnological reconstructions: a summary of examples from the Laurentian Great Lakes. *Org. Geochem.* 34, 261–289.

- Meyers, P., Ishiwatari, R., 1993. Lacustrine organic geochemistry—an overview of indicators of organic matter sources and diagenesis in lake sediments. *Org. Geochem.* 20, 867–900.
- Nobre, P., Shulka, J., 1996. Variations of sea surface temperature, wind stress and rainfall over the tropical Atlantic and South America. *J. Clim.* 9, 2464–2479.
- Novello, V.F., Cruz, F.W., Karmann, I., Burns, S.J., Strikis, N.M., Vuille, M., Cheng, H., Lawrence Edwards, R., Santos, R.V., Frigo, E., Barreto, E.A.S., 2012. Multidecadal climate variability in Brazil's Nordeste during the last 3000 years based on speleothem isotope records. *Geophys. Res. Lett.* 39, L23706.
- Pérez, M.C., Bonilla, S., Martínez, G., 1999. Phytoplankton community of a polymictic reservoir, La Plata river basin, Uruguay. *Rev. Bras. Biol.* 59 (4), 535–541.
- Peterson, L.C., Haug, G.H., 2006. Variability in the mean latitude of the Atlantic Intertropical Convergence Zone as recorded by riverine input of sediments to the Cariaco Basin (Venezuela). *Palaeogeogr. Palaeoclimatol. Palaeoecol.* 234, 97–113.
- Ran, L., Jiang, H., Knudsen, K.L., Eiriksson, J., 2011. Diatom-based reconstruction of palaeoceanographic changes on the North Icelandic shelf during the last millennium. *Palaeogeogr. Palaeoclimatol. Palaeoecol.* 302, 109–119.
- Reynolds, C.S., 1993. Scales of disturbance and their role in plankton ecology. *Hydrobiologia* 249, 157–171.
- Rodriguez, R.R., Haarsma, R.J., Campos, E.J.D., Ambrizzi, T., 2011. The impacts of inter-El Niño variability on the tropical Atlantic and Northeast Brazil climate. *J. Clim.* 24, 3402–3422.
- Ruhland, K.M., Smol, J.P., Pienitz, R., 2003. Ecology and spatial distributions of surface-sediment diatoms from 77 lakes in the subarctic Canadian treeline region. *Can. J. Bot.* 81, 57–73.
- Sifeddine, A., Albuquerque, A.L.S., Ledru, M.P., Turcq, B., Knoppers, B., Martin, L., de Mello, W. Z., Passenau, H., Dominguez, J.M.L., Cordeiro, R.C., Abrão, J.J., Bittencourt, A.C.S.P., 2003. A 21 000 cal years paleoclimatic record from Caçó Lake, northern Brazil: evidence from sedimentary and pollen analyses. *Palaeogeogr. Palaeoclimatol. Palaeoecol.* 189, 25–34.
- Sifeddine, A., Wirmann, D., Albuquerque, A.L.S., Turcq, B., Cordeiro, R.C., Gurgel, M.H.C., Abrão, J.J., 2004. Bulk composition of sedimentary organic matter used in palaeoenvironmental reconstructions: examples from the tropical belt of South America and Africa. *Palaeogeogr. Palaeoclimatol. Palaeoecol.* 214 (1–2), 41–45.
- Sifeddine, A., Gutiérrez, D., Ortlieb, L., Boucher, H., Velasco, F., Field, D., Vargas, G., Boussafir, M., Salvatelli, R., Ferreira, V., García, M., Valdés, J., Caquineau, S., Yogo, M.M., Cetin, F., Solis, J., Soler, P., Baumgartner, T., 2008. Laminated sediments from the central Peruvian continental slope: a 500 year record of upwelling system productivity, terrestrial runoff and redox conditions. *Prog. Oceanogr.* 79, 190–197.
- Stuiver, M., Reimer, P.J., 1993. *Radiocarbon* 35, 215–230.
- Sutton, R.T., Hodson, D.L.R., 2005. Atlantic Ocean forcing of North American and European summer climate. *Science* 309, 115–118.
- Tingstad, A.H., Moser, K.A., MacDonald, G.M., Munroe, J.S.A., 2011. ~13,000-year paleolimnological record from the Uinta Mountains, Utah, inferred from diatoms and loss-on-ignition analysis. *Quat. Int.* 235, 48–56.
- Turcq, B., Albuquerque, A.L.S., Cordeiro, R.C., Sifeddine, A., Simões Filho, F.F.L., Souza, A.G., Abrão, J.J., Oliveira, F.B.L., Silva, A.O., Capitâneo, J., 2002. Accumulation of organic carbon in five Brazilian lakes during the Holocene. *Sediment. Geol.* 148, 319–342.
- Velle, G., Telford, R.J., Heiri, O., Kurek, J., Birks, H.J.B., 2012. Testing intra-site transfer functions: an example using chironomids and water depth. *J. Paleolimnol.* 48, 545–558.
- Vuille, M., Burns, S.J., Taylor, B.L., Cruz, F.W., Bird, B.W., Abbot, M.B., Kanner, L.C., Cheng, H., Novello, V.F., 2012. A review of the South American monsoon history as recorded in stable isotopic proxies over the past two millennia. *Clim. Past* 8, 1309–1321.
- Wainer, I., Venegas, S., 2002. South Atlantic variability in the climate system model. *J. Clim.* 15, 1408–1420.
- Wang, C., Zhang, L., 2012. Multidecadal ocean temperature and salinity variability in the Tropical North Atlantic: linking with the AMO, AMOC, and Subtropical Cell. *J. Clim.* 26, 6137–6162.
- Watanabe, T., Winter, A., Oba, T., 2001. Seasonal changes in sea surface temperature and salinity during the Little Ice Age in the Caribbean Sea deduced from Mg/Ca and $^{18}\text{O}/^{16}\text{O}$ ratios. *Mar. Geol.* 173, 21–35.
- Zocatelli, R.O., Turcq, B., Boussafir, M., Cordeiro, R.C., Disnar, Jr., Lima da Costa, R.L., Sifeddine, A., Albuquerque, A.L.S., Bernardes, M.C., Jacob, J., 2012. Late Holocene paleoenvironmental changes in Northeast Brazil recorded by organic matter in lacustrine sediments of Lake Boqueirão. *Palaeogeogr. Palaeoclimatol. Palaeoecol.* 363–364, 127–134.